Sensors and Actuators B 182 (2013) 416–423

Contents lists available at SciVerse ScienceDirect

Sensors and Actuators B: Chemical

journal homepage: www.elsevier.com/locate/snb

Development of a field-portable fluorometer based on deep ultraviolet LEDs for the detection of phenanthrene- and tryptophan-like compounds in natural waters

Marc Tedetti[a,*], Pascal Joffre[b], Madeleine Goutx[a]

[a] Aix-Marseille Université, Mediterranean Institute of Oceanography (MIO), Université du Sud Toulon-Var, CNRS/INSU, IRD, UM 110, 13288 Marseille Cedex 09, France
[b] MicroModule, 38 rue Jim Sévellec, 29200 Brest, France

ARTICLE INFO

Article history:
Received 31 October 2012
Received in revised form 27 February 2013
Accepted 13 March 2013
Available online 23 March 2013

Keywords:
Field fluorometer
UV LED
Fluorescence
Phenanthrene
Tryptophan
Dissolved organic matter

ABSTRACT

In recent years, portable or submersible fluorometers have become key tools in acquiring real time high frequency measurements of target dissolved organic matter (DOM) fluorophores in aquatic environments. We have developed an original field-portable fluorometer based on deep UV light-emitting diodes (LEDs) for simultaneous measurements of two DOM fluorophores in natural waters: phenanthrene- and tryptophan-like compounds. This fluorometer, called "the MiniFluo-UV" was tested on standard solutions and natural samples collected on the northwestern Mediterranean coast (vicinity of Marseille City, France). The MiniFluo-UV responded linearly to an increase in phenanthrene and tryptophan concentrations over the range 0.1–100 $\mu g\,l^{-1}$. Limits of detection for these two fluorophores were 1.43 and 0.72 $\mu g\,l^{-1}$, respectively. The sensor also responded linearly to an increase in measurement duration over the range 200–2000 ms, and the fluorescence intensity showed a power decrease from calibre C0 (integration capacitor of 3 pF) to calibre C3 (integration capacitor of 73 pF). Optimal parameters (duration of 600 ms, calibre C0) were used for measurements in natural water samples. We found very significant linear relationships between the phenanthrene and tryptophan equivalent concentrations measured with the MiniFluo-UV and the concentrations measured with the Hitachi laboratory spectrofluorometer on all natural water samples (R^2 = 0.90 and 0.98, n = 150, $p < 0.01$). We conclude that the MiniFluo-UV fluorometer is a very relevant tool to detect and track sewage effluents and hydrocarbon contamination in marine coastal waters.

1. Introduction

For approximately two decades, fluorescence spectroscopy techniques, especially excitation–emission matrices (EEMs), have been fruitfully used to investigate the composition and dynamics of dissolved organic matter (DOM) in aquatic environments [1]. EEMs are produced over a range of excitation (λ_{Ex}) and emission (λ_{Em}) wavelengths from ~200 to 300 nm [deep-ultraviolet (UV) domain] to ~500–600 nm (visible domain) by means of sophisticated laboratory spectrofluorometers. The laboratory spectrofluorometers use a xenon lamp as the light source, a photomultiplier tube (PMT) as the sample light detector, a PMT or a silicon photodiode as the reference detector, and monochromators as light separators. EEMs have allowed the identification of two main types of fluorophores within the aquatic DOM pool: (1) protein-like fluorophores, with fluorescence signatures roughly similar to those of tryptophan ($\lambda_{Ex}/\lambda_{Em}$: ~225, 275/350 nm) and tyrosine aromatic amino acids ($\lambda_{Ex}/\lambda_{Em}$: ~ 225, 275/310 nm), generally attributed to autochthonous or labile DOM, and (2) humic-like fluorophores, with fluorescence signatures corresponding to those of humic ($\lambda_{Ex}/\lambda_{Em}$: 230–300/380–460 nm) and fulvic acids ($\lambda_{Ex}/\lambda_{Em}$: 320–380/400–500 nm), rather related to terrestrial or degraded DOM [2–5]. In addition to the protein- and humic-like fluorophores, anthropogenic DOM fluorophores may be found in natural waters, particularly polycyclic aromatic hydrocarbons (PAHs), which are highly fluorescent in the UV region ($\lambda_{Ex}/\lambda_{Em}$: 220–300/320–400 nm) [6–8].

Although EEMs remain the standard laboratory method to determine the fluorophore composition of DOM, they are fairly time-consuming because (1) they require that samples have to be brought from the field to the laboratory (with possible modification of samples during storage and transportation), and (2) they require an analysis time of 10–60 min. Recently, portable or submersible fluorometers have been employed to acquire rapid, real time, high frequency measurements of target DOM fluorophores in the aquatic media [9–11]. These fluorometers are equipped with a xenon lamp

* Corresponding author. Tel.: +33 4 91 82 90 62; fax: +33 4 91 82 90 51.
E-mail address: marc.tedetti@univ-amu.fr (M. Tedetti).

0925-4005/$ – see front matter © 2013 Elsevier B.V. All rights reserved.
http://dx.doi.org/10.1016/j.snb.2013.03.052

or a light-emitting diode (LED) as the light source, a silicon photodiode as the sample light detector (and as reference detector when present), and optical filters as light separators. For instance, the WETStar and ECO Puck submersible fluorometers (WETLabs Inc., USA) use a near-UV LED (300–400 nm) to measure a fulvic acid-like fluorophore at $\lambda_{Ex}/\lambda_{Em}$ of 370/460 nm [12,13]. The EnviroFlu-HC submersible fluorometer (TriOS Optical Sensors, Germany), which is equipped with a xenon lamp, has the capability of emitting λ_{Ex} in the deep UV (<300 nm) to detect phenanthrene, a typical PAH of petrogenic origin, at $\lambda_{Ex}/\lambda_{Em}$ of 254/360 nm [14]. The SMF handheld fluorometer (Safe Training Systems Ltd., UK) also has a xenon lamp to measure the tryptophan-like fluorophore at $\lambda_{Ex}/\lambda_{Em}$ of 280/360 nm [15].

Very recent advancements in semiconductor LED technology now offer the possibility of using deep UV LEDs in the range of 250–300 nm. The latter are based on aluminium gallium nitride (AlGaN) multiple quantum-well active layer designs and have continuous-wave output power in the 0.1–1 mW range at 20 mA driving current [16–18]. Due to their spectral selectivity, small size and weight, low power consumption, stability and low cost, deep UV LEDs present many advantages for fluorescence sensor applications compared to xenon lamps [19,20]. A deep UV LED at 280 nm currently replaces the xenon lamp in the new version of the SMF fluorometer to monitor the tryptophan-like fluorophore in diverse water samples [21].

We have developed an original field-portable fluorometer based on AlGaN deep-UV LEDs (255 and 280 nm) for simultaneous and rapid measurements of two groups of DOM fluorophores of interest in natural waters: phenanthrene- and tryptophan-like compounds. In this study, we report results obtained with this fluorometer, called "the MiniFluo-UV", on standard solutions and natural samples, and we demonstrate its usefulness as a monitoring tool for sewage effluents and PAH contamination in natural waters.

2. Materials and methods

2.1. Description of the MiniFluo-UV field-portable fluorometer

2.1.1. Mechanical and optical configurations

The MiniFluo-UV is in the form of a cylinder in a polyethylene housing resting on a square base (Ø × L: 70 × 200 mm; weight: 1000 g) (Fig. 1). Two cavities allow placing the two 1 cm pathlength deep UV silica quartz cuvettes (LEADER LAB®, France) containing the solutions dedicated to phenanthrene and tryptophan

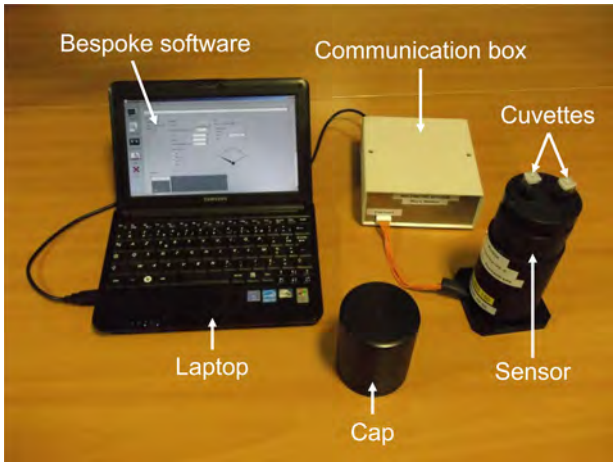

Fig. 1. Picture of the MiniFluo-UV field-portable fluorometer including the sensor itself, its cap, two quartz cuvettes placed in their respective cavity, the home-made communication box and the laptop running Windows® with bespoke software.

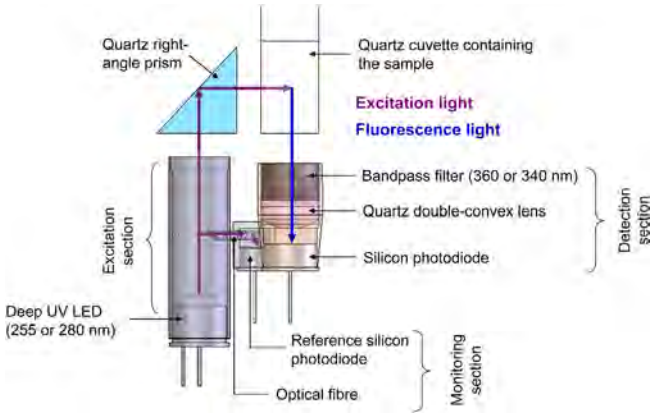

Fig. 2. Cutaway view of the MiniFluo-UV field-portable fluorometer, showing one optical channel (phenanthrene or tryptophan) with all optical components of each section, as well as the excitation and fluorescence light pathways.

fluorescence measurements. It is worth noting that the quartz cuvettes must have an optically polished bottom because the fluorescent light of solutions is collected by the sensor from the bottom of the cuvette (see the description of the optical configuration below). A cap (polyethylene housing) is placed on the top of the cylinder to perform the fluorescence measurements in the dark (Fig. 1).

The MiniFluo-UV has two optical channels for the simultaneous measurements of phenanthrene and tryptophan fluorophores. Each optical channel comprises one excitation section, one detection section, one monitoring section and one quartz right-angle prism (UV grade fused silica) (Fig. 2). Excitation sections and right-angle prisms are located on the central axis of the MiniFluo-UV, while detection and monitoring sections are situated on either side of this axis. Each section includes one or several specific optical components, integrated into a delrin or aluminium bushing and positioned vertically upward (Fig. 2).

The excitation section contains an AlGaN deep UV LED emitting at 255 nm (phenanthrene) or 280 nm (tryptophan). Emission spectra of the two LEDs were measured using a spectroradiometer. We found that the LED at 255 nm had a full-width half-maximum (FWHM) of 12 nm and an output power of 110 μW. On the other side, the LED at 280 nm had a FWHM of 12 nm and an output power of 630 μW. Photons emitted upward from the LEDs reach the right-angle prisms which redirect them towards the cuvettes to excitate phenanthrene and tryptophan molecules (Fig. 2).

The detection section, dedicated to the detection of phenanthrene and tryptophan fluorescent light emitted from the bottom of the cuvettes, incorporates a single-band bandpass filter centred at 360 (phenanthrene) or 340 nm (tryptophan), a quartz double-convex lens (UV grade fused silica), and a silicon photodiode (Fig. 2). Transmittance spectra of the bandpass filters were measured using a spectrophotometer. We found that the 360 nm filter had 90% transmittance at 360 nm and a FWHM of 16 nm, whereas the 340 nm filter had 90% transmittance at 340 nm and a FWHM of 18 nm. Another light detector was tested, the Multi-Pixel Photon Counter silicon photomultiplier, but the results were much less satisfactory than those obtained with the silicon photodiode (data not shown).

The monitoring section is used to monitor the photon flux emitted from the LEDs. A piece of optical fibre transfers a small amount of photons from the LED to a reference silicon photodiode (Fig. 2). If the LED photon flux varies with time, the fluorescence measurement may be corrected thanks to the monitoring measurement, the fluorescence intensity being directly proportional to the intensity

of the excitation light. Electronic circuits that manage this optical system are not described in this study.

2.1.2. Measurement parameters and data acquisition

The MiniFluo-UV, which uses an Inter Integrated Circuit (I^2C) serial communication mode, is operated with a home-made communication box and a laptop running Windows® (Fig. 1). The communication box allows the MiniFluo-UV to be powered by the laptop and to communicate with it through bespoke software (see below). The communication box includes a 32-bit PIC® microcontroller Ethernet starter kit associated with 10/100 Ethernet RJ-45 and USB micro-AB ports (Microchip Technology Inc., USA), a power over Ethernet extractor, and an USB voltage converter (5–12 V), which permits the supply of power and communication via USB or Ethernet. In this work, we used only the USB mode to run the MiniFluo-UV. Its power consumption was (on average) 500 mW at 12 V.

Bespoke software was developed especially for the MiniFluo-UV and its field/real-time applications. This software, programmed in C++, sends measurement parameters to the sensor as well as to acquiring, visualising and recording fluorescence data (Fig. 1). The measurement parameters that may be modified by the user comprise: (1) the LED functioning mode (OFF, ON or ON–OFF), (2) the calibre (C0–C3) and (3) the measurement duration (100–2000 ms) and (4) the sampling interval (100–10000 ms).

In the OFF mode (i.e., LEDs switched off), the photodiodes measure the level of ambient lighting (if the cap does not cover the MiniFluo-UV). In the ON mode (i.e., LEDs switched on), the photodiodes measure the fluorescence signal of molecules plus the level of ambient lighting. In ON–OFF mode, the photodiodes measure the fluorescence signal of molecules compensated for ambient lighting. The calibre corresponds to the integration capacitor of the analogue-to-digital converter of photodiodes. This integration capacitor [in pico farads (pF)] is inversely proportional to the output digital signal. Hence, the calibre from C0 (capacitor: 3 pF) to C3 (73 pF) is inversely proportional to the fluorescence intensity collected. The measurement duration (100–2000 ms) is the duration throughout which the LED is switched on and the fluorescence signal concomitantly recorded by the photodiode (synchronous functioning of LEDs and photodiodes). In ON–OFF mode, the measurement duration includes LEDs turned on half time and LEDs turned off half time. The sampling interval (100–10000 ms) is the time interval between two records, thus equal to or higher than the measurement duration.

The fluorescence data are acquired and displayed in real time in both numerical and graphical modes. Four values (unitless) come into sight simultaneously: two values corresponding to fluorescence intensities of phenanthrene and tryptophan, and two values associated with LED photon fluxes (monitoring data). Each measurement parameter (described above) is the same for these four output values. In addition to these fluorescence and monitoring data, ancillary parameters are available in real time: functioning duration (in s), internal temperature (in °C) and noise value (unitless). Data may be recorded in txt files. Start and stop of the recording are conducted by the user. Each recording displays six data columns: (1) time (in ms), (2) monitoring of the 255 nm LED, (3) fluorescence of phenanthrene, (4) monitoring of the 280 nm LED, (5) fluorescence of tryptophan and (6) internal temperature. Time between two lines is the sampling interval. The main characteristics of the MiniFluo-UV are summarised in Table 1.

2.2. Measurements on standard solutions

Measurements of standard solutions were performed in the laboratory under controlled conditions to assess the MiniFluo-UV response to phenanthrene and tryptophan fluorophores.

Table 1
Main characteristics of the MiniFluo-UV field-portable fluorometer.

Size (Ø × L)	70 mm × 200 mm
Weight	1000 g
Housing	Polyethylene
Excitation wavelengths	255 nm for phenanthrene, 280 nm for tryptophan
FWHM for excitation wavelengths	12 nm for phenanthrene and tryptophan
Emission wavelengths	360 nm for phenanthrene, 340 nm for tryptophan
FWHM for emission wavelengths	16 nm for phenanthrene, 18 nm for tryptophan
Communication mode	Integrated circuit (I^2C)
Power consumption	500 mW at 12 V
Measurement parameters	LED mode: OFF, ON or ON–OFF Calibre: C0 (3 pF), C1 (25 pF), C2 (50 pF), C3 (73 pF) Measurement duration: 100–2000 ms Sampling interval: 100–10000 ms
Data acquired	Time Monitoring of the LED at 255 nm Fluorescence of phenanthrene Monitoring of the LED at 280 nm Fluorescence of tryptophan Internal temperature

Phenanthrene and L-tryptophan were purchased from Sigma–Aldrich, USA (≥98%) and used without further purification. Standard solutions were prepared in ultrapure water, i.e. Milli-Q water from Millipore system, final resistivity 18.2 MΩ cm^{-1} at 25 °C, pH ∼ 5. Before being dissolved in water, phenanthrene was first dissolved in methanol (Suprasolv®, Merck, Germany). Standard solutions of phenanthrene and tryptophan ranged from 0.1 to 100 μg l^{-1}. The solutions were contained in 100 ml SCHOTT® glass bottles and stored in the dark at 4 °C for 48 h before analysis.

After 48 h, the standard solutions were allowed to reach 20 °C temperature in a dark thermostated room before being transferred into the quartz cuvettes and processed with the MiniFluo-UV. Tryptophan and phenanthrene solutions of same concentration were run at the same time in their respective (optical channel) cavity. For each solution, the measurement lasted 1 min. Several blanks (ultrapure water) were analysed before and after each set of standard solutions. All measurements were made in ON–OFF mode with various calibres and measurement durations. The sampling interval was always equal to the measurement duration. The series of measurements on standard solutions was repeated three times at intervals of several days. The average coefficient of variation for the three series was ∼10%.

2.3. Measurements on natural water samples

Marine and freshwater samples were collected on the northwestern Mediterranean coast, in the vicinity of Marseille City (south of France), from February to July 2011. Marine sites included two coastal stations ("Sofcom" and "Couronne"), two harbours ("Saumaty" and "Port-de-Bouc") and five stations located along a municipal sewage effluent outlet ("Cortiou"). These sites were sampled from the R/V Antédon II at ∼0.1 m and/or 5 m depth. Freshwater sites comprised a station in the Rhône River ("Rhône") and a station in the Vaccares Pond ("Vaccares"), sampled at ∼0.1 m depth. All these stations were sampled monthly, except Saumaty Harbour and the Cortiou stations, which were sampled once. Samples were collected in 100 ml SCHOTT® glass bottles. The latter were rinsed two times with the respective samples before filling, and stored in the dark at 4–8 °C.

Back in the laboratory, samples were filtered without delay under a low vacuum (<50 mm Hg) through pre-combusted GF/F (∼0.7 μm) glass fibre filters (25 mm diameter, Whatman). The

samples were allowed to reach the temperature of 20 °C, transferred into the quartz cuvettes and immediately processed with the MiniFluo-UV. Some samples were also analysed without being filtered (raw samples). Some measurements were carried out directly in the field to assess the feasibility of using the MiniFluo-UV as a portable fluorometer. For each sample, the two cuvettes were used for simultaneous detection of phenanthrene- and tryptophan-like fluorophores. As for standard solutions, the measurements lasted 1 min. Several blanks were analysed before and after each set of samples. All measurements were made in ON–OFF mode with fixed calibre and measurement duration, chosen according to the results obtained in the standard solutions. The sampling interval was equal to the measurement duration. All MiniFluo-UV data presented in this study [given in fluorescence raw counts (FRC) or in $\mu g\,l^{-1}$] are the means of fluorescence values acquired during the 1 min record. Coefficients of variation of these means were overall within the range 2–10%.

2.4. Spectral fluorescence analyses

Fluorescence measured by the MiniFluo-UV for standard solutions, filtered and raw natural samples was compared to that measured by a Hitachi (Japan) F-7000 laboratory spectrofluorometer. This instrument, which provides a measuring wavelength range of 200–750 nm on both excitation and emission sides, is equipped with a 150 W xenon short-arc lamp, two stigmatic concave diffraction gratings brazed at 300 (excitation side) and 400 nm (emission side) as single monochromators, and Hamamatsu R3788 PMTs as reference and sample detectors. The correction of spectra for the excitation and emission instrumental response was conducted from 200 to 600 nm according to the procedure recommended by Hitachi (Hitachi F-7000 Instruction Manual) and fully described in [22].

Samples were transferred to a deep UV silica cuvette (one of those used for the MiniFluo-UV), which was thermostated at 20 °C in the spectrofluorometer cell holder by an external circulating water bath. EEMs were generated over λ_{Ex} between 200 and 500 nm in 5 nm intervals and λ_{Em} between 280 and 550 nm in 2 nm intervals, with 5 nm FWHMs on both excitation and emission sides, a scan speed of 1200 nm min^{-1}, a time response of 500 ms and a PMT voltage of 700 V. Blanks (ultrapure water) were regularly run and the water Raman scatter peak was monitored at $\lambda_{Ex}/\lambda_{Em}$ of 275/303 nm. Although absorbance measurements were carried out from 200 to 600 with a Shimadzu UV-Vis 2450 spectrophotometer, no correction for inner filtering effects was applied in this work, neither for spectrofluorometer measurements, nor for MiniFluo-UV measurements.

3. Results and discussion

3.1. Response of the MiniFluo-UV to standard solutions

Fig. 3 shows EEM contour plots of phenanthrene and tryptophan fluorophores in ultrapure water, upon which is placed the measurement spectral domain of the MiniFluo-UV. We can see that phenanthrene and tryptophan displayed distinct fluorescence signatures, with peaks at $\lambda_{Ex}/\lambda_{Em}$ of 250/364 and 275/352 nm, respectively. Tryptophan had a second fluorescence peak at $\lambda_{Ex}/\lambda_{Em}$ of 220/352 nm, which is not visible on this figure (see this second peak in [3,14]). Phenanthrene, with a peak intensity of 750 FRC at 10 $\mu g\,l^{-1}$, was much more fluorescent than tryptophan, which had a peak intensity of 240 FRC at 20 $\mu g\,l^{-1}$. Indeed, phenanthrene is composed of three fused benzene rings, while tryptophan presents an indole group, i.e., a fused benzene ring plus a nitrogen-containing pyrrole ring (Fig. 3). The degree of conjugation (alternating single and double bonds) and, subsequently, the fluorescence quantum yield is thus higher for phenanthrene than for tryptophan [23,24]. The match between the fluorophore fluorescence domain and the MiniFluo-UV measurement domain was better for phenanthrene ($\lambda_{Ex}/\lambda_{Em}$ of 250/364 and 255/360 nm, respectively) than for tryptophan ($\lambda_{Ex}/\lambda_{Em}$ of 275/352 and 280/340 nm, respectively) (Fig. 3). However, the tryptophan-like fluorophore present in natural water samples has a blue-shifted fluorescence emission wavelength compared to tryptophan standard, and thus, a fluorescence domain superimposed perfectly on the spectral domain of the tryptophan optical channel (see Section 3.2).

The MiniFluo-UV responded linearly to an increase in phenanthrene and tryptophan concentrations over the range 0.1–100 $\mu g\,l^{-1}$ for fixed calibre (C0) and measurement duration (600 ms) ($R^2 = 1.00$, $n = 8$, $p < 0.01$; Fig. 4a and b). The instrument exhibited a lower sensitivity for phenanthrene (slope of the regression curve: 663 FRC/$\mu g\,l^{-1}$) than for tryptophan (slope: 925 FRC/$\mu g\,l^{-1}$). The sensor blank value (y-intercept of the regression curve) was higher for phenanthrene (6471 FRC) than for tryptophan (3511 FRC) (Fig. 4a and b). Consequently, the MiniFluo-UV was less efficient in the detection of phenanthrene than in the detection of tryptophan, with limits of detection (LOD) of 1.43 and 0.72 $\mu g\,l^{-1}$, respectively. This result seems rather surprising

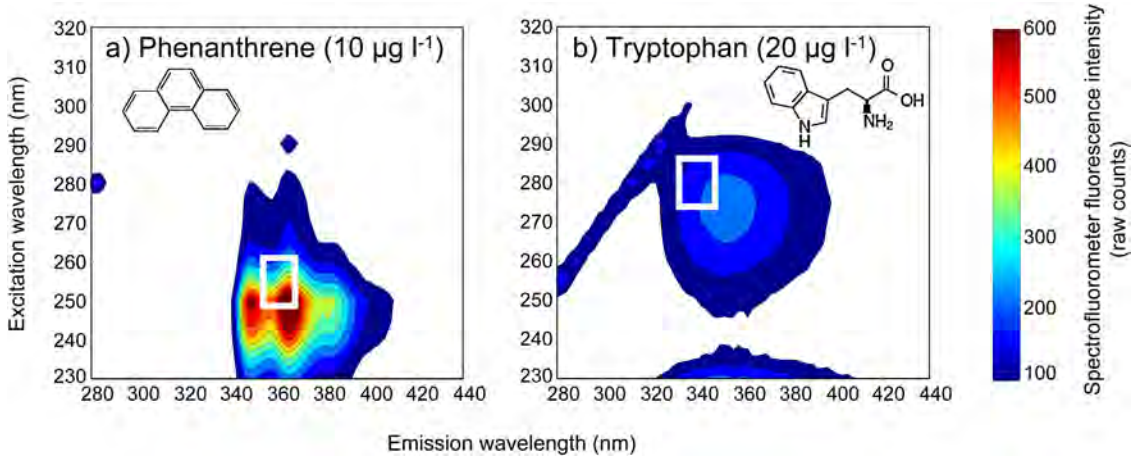

Fig. 3. Excitation–emission matrix (EEM) contour plots of standard fluorophores in ultrapure water, upon which is placed the measurement spectral domain of the MiniFluo-UV field-portable fluorometer (white rectangle): (a) standard phenanthrene at 10 $\mu g\,l^{-1}$ and spectral domain of the phenanthrene optical channel ($\lambda_{Ex}/\lambda_{Em}$: 255/360 nm; FWHMs: 12/16 nm) and (b) standard tryptophan at 20 $\mu g\,l^{-1}$ and spectral domain of the tryptophan optical channel ($\lambda_{Ex}/\lambda_{Em}$: 280/340 nm; FWHMs: 12/18 nm). Chemical structures of phenanthrene and tryptophan are also presented. EEMs were obtained from a Hitachi laboratory spectrofluorometer.

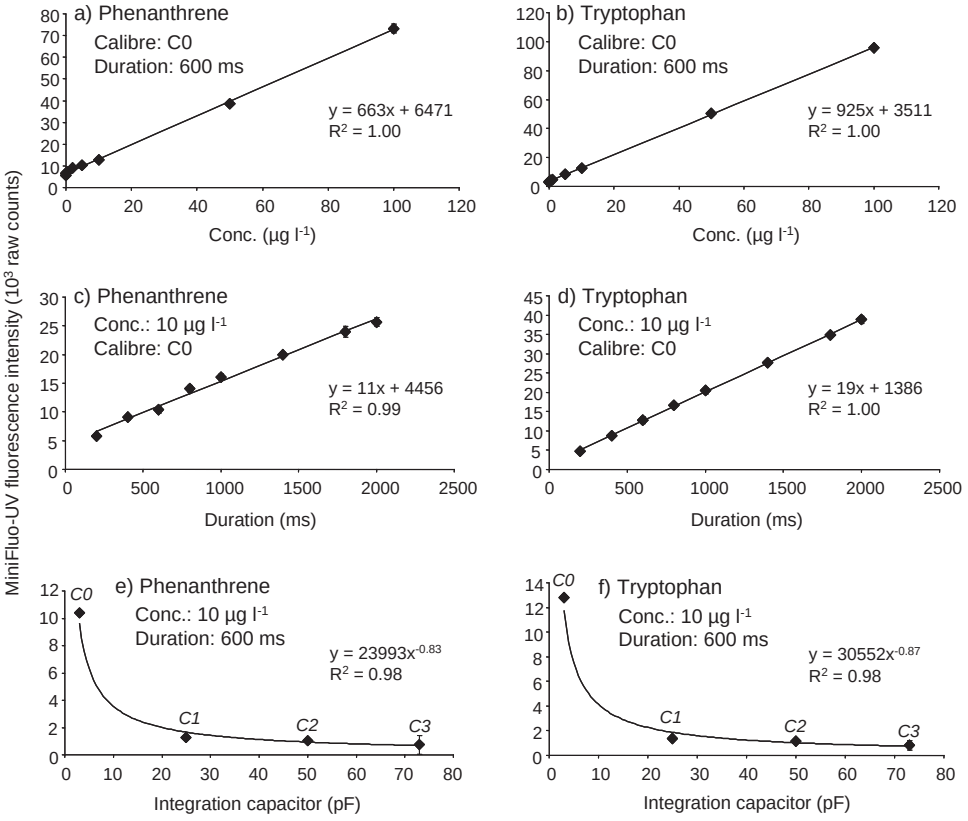

Fig. 4. Calibration of the MiniFluo-UV field-portable fluorometer with standard fluorophores in ultrapure water: relationships between the MiniFluo-UV fluorescence intensity and (a and b) the fluorophore concentration (0.1–100 µg l^{-1}) with fixed calibre (C0) and measurement duration (600 ms), (c and d) the measurement duration (200–2000 ms) with fixed fluorophore concentration (10 µg l^{-1}) and calibre (C0), and (e and f) the calibre (C0–C3, corresponding to the integration capacitor 3–73 pF) with fixed fluorophore concentration (10 µg l^{-1}) and measurement duration (600 ms). Phenanthrene and tryptophan fluorophores were measured with their respective optical channel. All measurements were performed in ON–OFF LED mode. The sampling interval was equal to the measurement duration.

relative to the fluorescence properties of fluorophores (phenanthrene much more fluorescent than tryptophan, see previous paragraph), but becomes rational when considering the performances of the two MiniFluo-UV optical channels. As mentioned in Section 2.1.1, the output power of the LED at 255 nm dedicated to phenanthrene measurement (110 µW) was much lower than the output power of the LED at 280 nm used for tryptophan (630 µW). Because there were no differences in the performance of the optical components from the detection sections (filters, photodiodes), this discrepancy in the excitation light intensities may explain the lower response for phenanthrene entirely. LOD of phenanthrene and tryptophan determined from the same standard solutions analysed on the Hitachi spectrofluorometer were 0.21 and 0.39 µg l^{-1}, respectively (calibration curves not shown). In this case, owing to the application of excitation (and emission) instrumental corrections, an inverse pattern occurred with a better detection found for phenanthrene. Interestingly, the LOD obtained from the MiniFluo-UV and those acquired from the spectrofluorometer differed by a factor 6.8 (phenanthrene) and 1.8 (tryptophan), which emphasises the quite good capabilities of our field fluorometer.

The MiniFluo-UV responded linearly to an increase in measurement duration over the range 200–2000 ms for fixed fluorophore concentration (10 µg l^{-1}) and calibre (C0) (R^2 = 0.99 and 1.00, n = 8, p < 0.01; Fig. 4c and d). As expected, the longer the measurement duration, the higher the fluorescence intensity. In accordance with results in Fig. 4a and b, we observed that the MiniFluo-UV sensitivity was lower for phenanthrene (slope of the regression curve: 11 FRC/ms) than for tryptophan (slope: 19 FRC/ms) (Fig. 4c and d). Finally, the MiniFluo-UV fluorescence intensity showed a power decrease from calibre C0 (integration capacitor of 3 pF) to calibre C3 (integration capacitor of 73 pF) for fixed fluorophore concentration (10 µg l^{-1}) and measurement duration (600 ms) (R^2 = 0.98, n = 4, p < 0.05; Fig. 4e and f). Although this decrease was predictable (integration capacitor inversely proportional to the sensor output signal), we would have expected a linear diminution. This power decrease was very likely related to some variations in the integration capacitor values recorded in the sensor firmware. From these results (Fig. 4c–f), we may conclude that the MiniFluo-UV optimal parameters for the detection of the two fluorophores were calibre C0 and measurement duration of 2000 ms. When performing calibration with a measurement duration of 2000 ms (figures not shown), we obtained an LOD of 1.10 and 0.68 µg l^{-1} for phenanthrene and tryptophan, respectively. This values represent an improvement compared to the LOD acquired with the 600 ms duration (1.43 and 0.72 µg l^{-1}, respectively; Fig. 4a and b). Nevertheless, the difference was not significant because the 2000 ms duration generated much more important leakage currents leading to a high noise level (i.e., high y-intercept values in the regression curves), which limited accuracy at the lowest concentrations. Therefore, for measurements carried out on natural water samples (Section 3.2), we decided to use a measurement duration of 600 ms with calibre C0.

3.2. Response of the MiniFluo-UV to natural water samples

We found very significant linear relationships between the phenanthrene and tryptophan equivalent concentrations measured with the MiniFluo-UV and those measured with the Hitachi spectrofluorometer on all (filtered and raw) natural water samples (R^2 = 0.90 and 0.98, n = 150, p < 0.01; Fig. 5a and b). The correlation

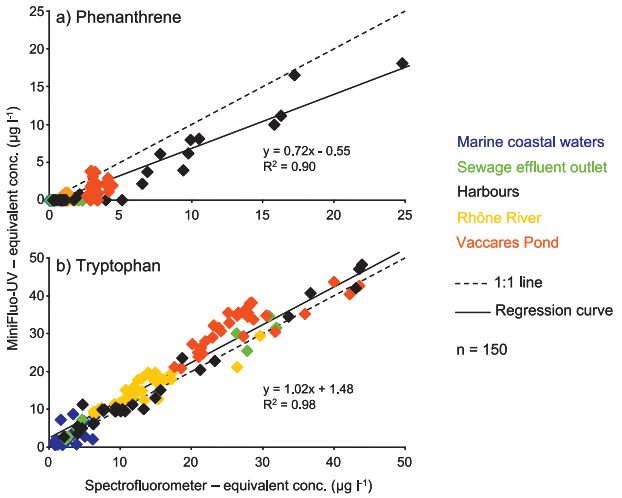

Fig. 5. Comparison between the phenanthrene and tryptophan equivalent concentrations measured with the MiniFluo-UV field-portable fluorometer and those measured with the Hitachi laboratory spectrofluorometer on all (filtered and raw) natural water samples ($n = 150$). The MiniFluo-UV measurements were carried out in ON–OFF LED mode, with the calibre C0, and a measurement duration and a sampling interval of 600 ms. The phenanthrene and tryptophan equivalent concentrations in $\mu g\,l^{-1}$ were determined by using the equations of linear regression curves reported in Fig. 4a and b. For the spectrofluorometer, the fluorescence intensities of phenanthrene and tryptophan were recovered from excitation–emission matrices (EEMs) at $\lambda_{Ex}/\lambda_{Em}$ of 255/360 nm and $\lambda_{Ex}/\lambda_{Em}$ of 280/340 nm, respectively, and the equivalent concentrations in $\mu g\,l^{-1}$ were determined by using the appropriate equations of linear regression curves.

was, however, of worse quality for phenanthrene. For the latter, the concentrations determined from the MiniFluo-UV were systematically lower than those issued from the spectrofluorometer (slope of the regression curve: 0.72). Moreover, for phenanthrene concentrations measured with the spectrofluorometer lower than 3 $\mu g\,l^{-1}$, the MiniFluo-UV was not able to detect a phenanthrene-like compound (Fig. 5a). These results are in accordance with those derived from phenanthrene standard solutions, which noted a difference by a factor 6.8 in the LOD of the two instruments. We can see that the highest phenanthrene concentrations were found in harbours (up to 25 $\mu g\,l^{-1}$). Phenanthrene-like compound was also present in the Vaccares Pond in the range 3–4.5 $\mu g\,l^{-1}$, was weakly present in the Rhône River and Cortiou sewage effluent outlet (0.2–2.3 $\mu g\,l^{-1}$), and was totally absent in marine coastal waters (Fig. 5a). Concerning tryptophan, the concentrations determined from the MiniFluo-UV were identical to the concentrations recovered from the spectrofluorometer (slope of the regression curve: 1.02). For both fluorometers, tryptophan-like compound was detected at concentrations as low as 0.5 $\mu g\,l^{-1}$ (Fig. 5b). These results are in agreement with those obtained on tryptophan standard solutions, which underlined very close LODs for the two instruments. Contrary to what was observed for phenanthrene, the tryptophan-like compound was present in all water bodies, including marine coastal waters, with the highest concentrations encountered in harbours, Vaccares Pond (up to 44 $\mu g\,l^{-1}$) and Cortiou sewage effluent outlet (up to 32 $\mu g\,l^{-1}$) (Fig. 5b).

Undoubtedly, the phenanthrene- and tryptophan-like fluorescence signals measured in these diverse natural water samples by the MiniFluo-UV at $\lambda_{Ex}/\lambda_{Em}$ of 255/360 and 280/340 nm, respectively, were not always attributable to "true" phenanthrene- and tryptophan-like fluorophores. Fig. 6 depicts EEM contour plots of raw marine water samples, upon which are placed the two measurement spectral domains of the MiniFluo-UV. In the vicinity of the Cortiou sewage effluent outlet, we detected the presence of tryptophan-like fluorophore with a peak at $\lambda_{Ex}/\lambda_{Em}$ of 280/342 nm, perfectly superimposed on the spectral domain of the tryptophan optical channel (Fig. 6a). In sewage effluent-impacted natural waters, tryptophan-like fluorophore is usually one of the most abundant DOM fluorophores [15,22], derived from sewage microbial activity and well correlated with biological oxygen demand [21,25]. The tryptophan-like fluorophore of natural waters is known to have a blue-shifted fluorescence emission wavelength compared to tryptophan pure standard (comparison Fig. 6a and Fig. 3b), very likely because it is bound in proteins or organism cell walls [26]. On the other hand, phenanthrene-like compound at $\lambda_{Ex}/\lambda_{Em}$ of 255/360 nm was actually not present at the Cortiou sewage effluent outlet (Fig. 6a). Tryptophan equivalent concentrations measured with the MiniFluo-UV at the five stations along the Cortiou sewage effluent outlet are provided in Fig. 7a. A marked decrease in tryptophan concentrations occurred from in shore (40 m from the outlet, 32 $\mu g\,l^{-1}$) to offshore waters (at 1.5 km from the outlet, 2.4 $\mu g\,l^{-1}$). This decrease reflected the extent of the sewage effluent dilution plume in marine coastal waters.

In Saumaty Harbour, the tryptophan-like signal measured by the sensor at $\lambda_{Ex}/\lambda_{Em}$ of 280/340 nm was not merely attributable to the tryptophan-like fluorophore (Fig. 6b). The application of parallel factor analysis (PARAFAC) on the harbour dataset, not detailed here, resulted in the identification of two fluorophores around the spectral domain of the tryptophan optical channel: one fluorophore

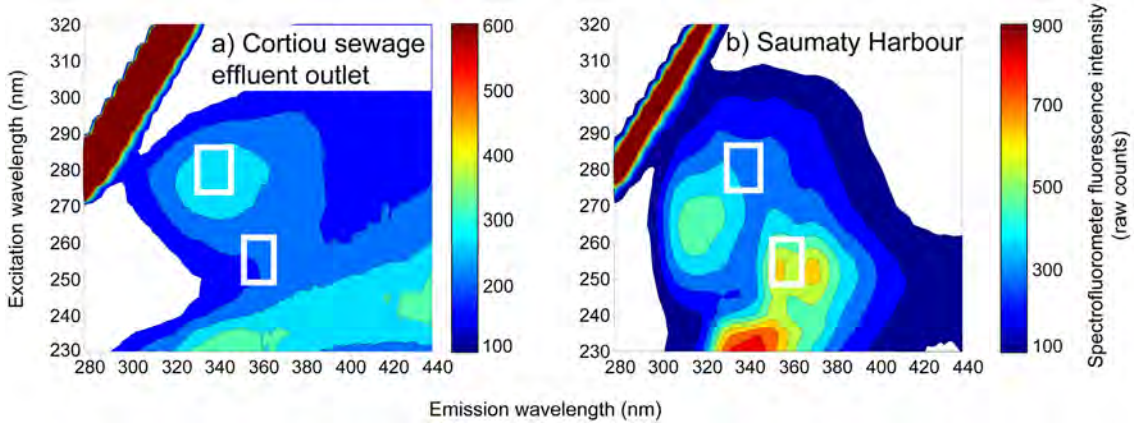

Fig. 6. Excitation–emission matrix (EEM) contour plots of raw marine water samples collected in the northwestern Mediterranean coast (vicinity of Marseille City), upon which are placed the two measurement spectral domains of the MiniFluo-UV field-portable fluorometer (white rectangles): (a) Cortiou sewage effluent outlet and (b) Saumaty Harbour. The white rectangles are the spectral domains of the phenanthrene ($\lambda_{Ex}/\lambda_{Em}$: 255/360 nm; FWHMs: 12/16 nm) and tryptophan optical channels ($\lambda_{Ex}/\lambda_{Em}$: 280/340 nm; FWHMs: 12/18 nm). EEMs were obtained from a Hitachi laboratory spectrofluorometer.

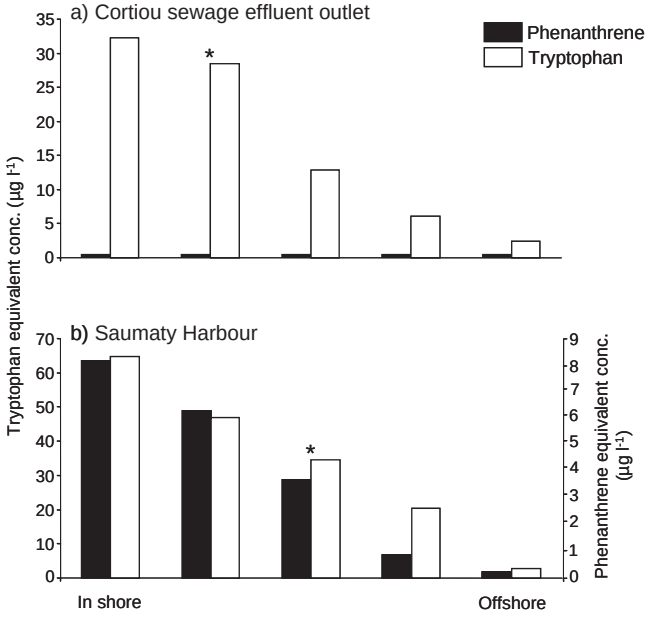

Fig. 7. Phenanthrene and tryptophan equivalent concentrations measured with the MiniFluo-UV field-portable fluorometer at two sites of the northwestern Mediterranean coast (vicinity of Marseille City) from in shore to offshore waters: (a) Cortiou sewage effluent outlet and (b) Saumaty Harbour. Asterisks indicate the (raw) samples for which excitation–emission matrix (EEM) contour plots are displayed in Fig. 6. The MiniFluo-UV measurements were carried out in ON–OFF LED mode, with the calibre C0, and a measurement duration and a sampling interval of 600 ms. The phenanthrene and tryptophan equivalent concentrations in $\mu g\,l^{-1}$ were determined by using the equations of linear regression curves reported in Fig. 4a and b.

with a peak at $\lambda_{Ex}/\lambda_{Em}$ of 265/316 nm, clearly visible on Fig. 6b, and a tryptophan-like fluorophore with its peak at $\lambda_{Ex}/\lambda_{Em}$ of 280/340 nm, partially hidden on the figure. By comparing the excitation and emission spectra of the unidentified fluorophore with those of several standard PAHs and by comparing its fluorescence intensities with PAH concentrations determined by chromatographic analyses (GC/MS) on the same samples, we determined that this fluorophore was fluorene (Ferreto et al., unpublished). Therefore, in Saumaty Harbour, the MiniFluo-UV tryptophan-like signal was due to both tryptophan- and fluorene-like fluorophores. The phenanthrene-like signal measured by the MiniFluo-UV at $\lambda_{Ex}/\lambda_{Em}$ of 255/360 nm was fully derived from the phenanthrene compound, which displayed its peak at $\lambda_{Ex}/\lambda_{Em}$ of 250/370 nm (Fig. 6b). This identification was confirmed by the correlation between the fluorescence intensities and phenanthrene concentrations determined by GC/MS. Like phenanthrene, fluorene is a major PAH in the aquatic environment and is highly fluorescent [27–29]. Phenanthrene and tryptophan equivalent concentrations recorded with the MiniFluo-UV decreased substantially in Saumaty Harbour from in shore (inside the harbour, 8.1 and 66 $\mu g\,l^{-1}$, respectively) to offshore waters (at 0.5 km from the harbour, 0.3 and 2.7 $\mu g\,l^{-1}$, respectively) (Fig. 7b). This gradient underscored the extent of the PAH contamination in marine coastal waters.

4. Conclusions and perspectives

This work highlights the performance of the MiniFluo-UV field-portable fluorometer for the detection of phenanthrene- and tryptophan-like compounds in natural waters. This sensor is an inexpensive, low consumption sensor suitable for real-time processes and field applications. Owing to numerous user-settable calibres and LED pulse durations, the MiniFluo-UV possesses unique measurement dynamics with limits of detection for target fluorophores in the $\mu g\,l^{-1}$ range. As shown here, this sensor is relevant to detect and track sewage effluents and PAH contamination in marine coastal waters. Improvements are currently being undertaken to increase the sensitivity of the two optical channels, particularly the optical channel dedicated to phenanthrene measurement (LED at 255 nm). A submersible version of the MiniFluo-UV has been built and is being tested at sea. This submersible sensor may integrate different underwater platforms such as CTD profilers, profiling floats and gliders.

Acknowledgments

We are grateful to the captain and crew of the R/V Antédon II for their excellent cooperation. We acknowledge N. Ferretto for the field measurements and sampling. We also thank anonymous reviewers for their helpful comments. This study is a contribution of SEA EXPLORER and VASQUE projects (leader: ACSA-ALCEN, Meyreuil, France), which aim at developing autonomous underwater vehicles (gliders) for operational oceanography and urban marine zone management. These projects are labelled by the Competitivity Cluster Mer PACA. SEA EXPLORER was supported by the Fonds unique interministériel (FUI) and VASQUE was funded by the direction générale de la compétitivité, de l'industrie et des services (DGCIS) – Eco industries program. This work also received the financial support of the Agence Nationale de la Recherche (ANR) – ECOTECH program (project IBISCUS: ANR-09-ECOT-009-01).

References

[1] P.G. Coble, Characterization of marine and terrestrial DOM in seawater using excitation–emission matrix spectroscopy, Marine Chemistry 51 (1996) 325–346.
[2] P.G. Coble, Marine optical biogeochemistry – the chemistry of ocean color, Chemical Reviews 107 (2007) 402–418.
[3] N. Hudson, A. Baker, D. Reynolds, Fluorescence analysis of dissolved organic matter in natural, waste and polluted waters – a review, River Research and Applications 23 (2007) 631–649.
[4] J.B. Fellman, E. Hood, R.G.M. Spencer, Fluorescence spectroscopy opens new windows into dissolved organic matter dynamics in freshwater ecosystems: a review, Limnology and Oceanography 55 (2010) 2452–2462.
[5] S.K.L. Ishii, T.H. Boyer, Behavior of reoccurring PARAFAC components in fluorescent dissolved organic matter in natural and engineered systems: a critical review, Environmental Science and Technology 46 (2012) 2006–2017.
[6] A. Baker, M. Curry, Fluorescence of leachates from three contrasting landfills, Water Research 38 (2004) 2605–2613.
[7] K.R. Murphy, G.M. Ruiz, W.T.M. Dunsmuir, T.D. Waite, Optimized parameters for fluorescence-based verification of ballast water exchange by ships, Environmental Science and Technology 40 (2006) 2357–2362.
[8] M.L. Nahorniak, K.S. Booksh, Excitation–emission matrix fluorescence spectroscopy in conjunction with multiway analysis for PAH detection in complex matrices, Analyst 131 (2006) 1308–1315.
[9] R.N. Conmy, P.G. Coble, C.E. Del Castillo, Calibration and performance of a new in situ multi-channel fluorometer for measurement of colored dissolved organic matter in the ocean, Continental Shelf Research 24 (2004) 431–442.
[10] C. Moore, A. Barnard, P. Fietzek, M.R. Lewis, H.M. Sosik, S. White, O. Zielinski, Optical tools for ocean monitoring and research, Ocean Science 5 (2009) 661–684.
[11] O. Zielinski, J.A. Busch, A.D. Cembella, K.L. Daly, J. Engelbrektsson, A.K. Hannides, H. Schmidt, Detecting marine hazardous substances and organisms: sensors for pollutants, toxins, and pathogens, Ocean Science 5 (2009) 329–349.
[12] C. Belzile, C.S. Roesler, J.P. Christensen, N. Shakhova, I. Semiletov, Fluorescence measured using the WETStar DOM fluorometer as a proxy for dissolved matter absorption, Estuarine, Coastal and Shelf Science 67 (2006) 441–449.
[13] K. Niewiadomska, H. Claustre, L. Prieur, F. D'Ortenzio, Submesoscale physical–biogeochemical coupling across the Ligurian current (northwestern Mediterranean) using a bio-optical glider, Limnology and Oceanography 53 (2008) 2210–2225.
[14] M. Tedetti, C. Guigue, M. Goutx, Utilization of a submersible UV fluorometer for monitoring anthropogenic inputs in the Mediterranean coastal waters, Marine Pollution Bulletin 60 (2010) 350–362.
[15] A. Baker, D. Ward, S.H. Lieten, R. Periera, E.C. Simpson, M. Slater, Measurement of protein-like fluorescence in river and waste water using a handheld spectrophotometer, Water Research 38 (2004) 2934–2938.
[16] W.H. Sun, J.P. Zhang, V. Adivarahan, A. Chitnis, M. Shatalov, S. Wu, V. Mandavilli, J.W. Yang, M.A. Khan, AlGaN-based 280 nm light-emitting diodes with continuous wave powers in excess of 1.5 mW, Applied Physics Letters 85 (2004) 531–533.

[17] J.P. Zhang, X. Hu, Yu. Bilenko, J. Deng, A. Lunev, M.S. Shur, R. Gaska, M. Shatalov, J.W. Yang, M.A. Khan, AlGaN-based 280 nm light-emitting diodes with continuous-wave power exceeding 1 mWat 25 mA, Applied Physics Letters 85 (2004) 5532–5534.
[18] M. Belz, F.A. Klein, H.S. Eckhardt, K.F. Klein, D. Dinges, K.T.V. Grattan, Optical detection techniques and light delivery with UV LEDs and optical fibres third international conference on optical and laser diagnostics, Journal of Physics: Conference Series 85 (2007) 012034.
[19] N. Ryškeviĉ, S. Jeršėnas, P. Vitta, E. Bakienė, R. Gaska, A. Žukauskas, Concept design of a UV light-emitting diode based fluorescence sensor for real-time bioparticle detection, Sensors and Actuators B – Chemical 148 (2010) 371–378.
[20] J.E. Dickens, M.S. Vaughn, M. Taylor, M. Ponstingl, An LED array-based light induced fluorescence sensor for real-time process and field monitoring, Sensors and Actuators B – Chemical 158 (2011) 35–42.
[21] S. Cumberland, J. Bridgeman, A. Baker, M. Sterling, D. Ward, Fluorescence spectroscopy as a tool for determining microbial quality in potable water applications, Environmental Technology (2011) 588401, http://dx.doi.org/10.1080/09593330.2011.
[22] M. Tedetti, R. Longhitano, N. Garcia, G. Guigue, N. Ferretto, M. Goutx, Fluorescence properties of dissolved organic matter in coastal Mediterranean waters influenced by a municipal sewage effluent (Bay of Marseilles, France), Environmental Chemistry 9 (2012) 438–449.
[23] J.R. Lakowicz, Principle of Fluorescence Spectroscopy, second ed., Kluwer Academic/Plenum Publishers, New York, 1999725.
[24] A.M. Brouwer, Standards for photoluminescence quantum yield measurements in solution (IUPAC Technical Report), Pure and Applied Chemistry 83 (2011) 2213–2228.
[25] S.R. Ahmad, D.M. Reynolds, Monitoring of water quality using fluorescence technique: prospect of on-line process control, Water Research 33 (1999) 2069–2074.
[26] S. Determann, J.M. Lobbes, R. Reuter, J. Rullkötter, Ultraviolet fluorescence excitation and emission spectroscopy of marine algae and bacteria, Marine Chemistry 62 (1998) 137–156.
[27] J.L. Beltrán, R. Ferrer, J. Guiteras, Multivariate calibration of polycyclic aromatic hydrocarbon mixtures from excitation–emission fluorescence spectra, Analytica Chimica Acta 373 (1998) 311–319.
[28] F. Telli-Karakoç, L. Tolun, B. Henkelmann, C. Klimm, O. Okay, K.W. Schramm, Polycyclic aromatic hydrocarbons (PAHs) and polychlorinated biphenyls (PCBs) distributions in the Bay of Marmara Sea: İzmit Bay, Environmental Pollution 119 (2002) 383–397.
[29] A. El Nemr, A.M.A. Abd-Allah, Contamination of polycyclic aromatic hydrocarbons (PAHs) in microlayer and subsurface waters along Alexandria coast, Egypt, Chemosphere 52 (2003) 1711–1716.

Biographies

Marc Tedetti received his PhD degree in marine biogeochemistry from the University of Méditerranée (Marseille, France), in collaboration with Hokkaido University (Sapporo, Japan), in 2006. He is currently holding a postdoctoral position at the Mediterranean Institute of Oceanography (MIO, Marseille). His main research interests concern the dynamics of dissolved organic matter and organic pollutants in coastal environments through the use of spectroscopic (fluorescence) and geochemical techniques.

Pascal Joffre, physicist engineer from the Institut National de Polytechnique de Grenoble, is manager of the company "MicroModule" (Brest, France). This company specialises in the development of optical devices, opto-electronic systems and environmental sensors.

Madeleine Goutx is director of research at Centre National de la Recherche Scientifique (CNRS) at the Mediterranean Institute of Oceanography (MIO, Marseille). She has strong expertise in the study of anthropogenic tracers, lipid biomarkers, PAHs and hydrocarbons, fluorescent dissolved organic matter (FDOM) and bacterial lipase activities in the marine environment.